Dynamic compressive behavior of a novel ultra-lightweight cement composite incorporated with rubber powder

Zhenyu HUANG[1,2], Lili SUI[1,2*], Fang WANG[1,2], Shilin DU[2], Yingwu ZHOU[1,2], Jianqiao YE[3*]

1 Guangdong Provincial Key Laboratory of Durability for Marine Civil Engineering, Shenzhen University, Shenzhen, China 518060.

2 College of Civil and Transportation Engineering, Shenzhen University, Shenzhen, China 518060.

3 Department of Engineering, Lancaster University, Lancaster LA1 4YR, UK

Abstract

This paper develops a novel rubberized ultra-lightweight high ductility cement composite (RULCC) with added rubber powder and low content PE fiber (0.7%), and investigates the dynamic compressive response and failure mechanism of the RULCC both experimentally and analytically. The test program examines the dynamic compressive stress-strain relationship of the RULCC through Split Hopkinson Pressure Bar (SHPB) impact tests. The results show that the rubber powder aggregates have significant effect on the compressive strength, stress-strain relations and failure mechanism of the RULCC. A volume replacement of fine aggregates with 5%, 10% and 20% rubber power results in a reduction in static compressive strength by 29.5%, 47.7% and 60.3%, respectively. The RULCC with a low fiber content of 0.7% in volume exhibits a 3% direct tensile strain, and a 4-5% tensile strain can still be achieved after 10% rubber powder is added to the RULCC, showing a high ductility of the material. The SHPB impact test shows that the compressive strength increases with strain rate. An empirical model, taking into account of the replacement ratio of the rubber powder aggregates in the RULCC, is developed in this paper to evaluate the Dynamic Increasing Factor (DIF). The experimental and analytical studies are essential to better understand the fundamental dynamic behavior of the RULCC for its further applications in engineering applications, such as protective structures, etc.

Keywords**:** Rubberized concrete; Cement composite; Lightweight Concrete; Split Hopkinson Pressure Bar.

* Corresponding author. Tel: +86 755-86975402; Fax: +86 755-26732850; Emails: suill@szu.edu.cn; j.ye@lancaster.ac.uk

1. Introduction

Concrete using lightweight aggregates, such as expanded clay/shale [1], fly ash aggregates [2], fly ash cenospheres [3, 4], perlite [5], pumice [6], are classified as Lightweight aggregate concrete (LWAC). As summarized in Huang et al [4], LWAC has an apparent density of less than, e.g., 2000 kg/m^3 with a compressive strength of 8-80MPa, 1950kg/m^3 with a compressive strength of 10-38.5MPa and 1850 kg/m^3 with a compressive strength of 17-35MPa, respectively, as specified in JGJ 51-2002 [7], CEB-FIP 2010 and BS EN 13055-2016 [8,9], ACI 213R-14 and ASTM C330 [10, 11]. Lightweight aggregates mainly reduce self-weight and improve thermal performance of concrete [12, 13]. LWAC can be used in industrial and building structures to reduce structural weight and the materials used in construction. LWAC also reduces the transportation and hoisting cost during construction, the gravity load on the foundation, thus the reinforcement and labor cost [1-6, 12-15]. Due to the superior performance of LWAC, it has been used in, e.g., bridges [16], prefabricated construction [17] and offshore structures [18]. To further reduce the self-weight of offshore structures, Huang et al. [3, 4], Chia et al. [19] and Wu et al. [20] developed a novel ultra-lightweight cement composite (ULCC) using fly ash cenospheres. The apparent density of the ULCC is only 1450kg/m^3 with a 28-day compressive strength of 60MPa. To further downsize the design, they developed a novel steel-ULCC-steel sandwich composite [21], and studied the bending, shearing, compression and dynamic impact resistance of beams, plates, shells and walls made of the sandwich composite experimentally and theoretically [15,18,21-24]. A set of design methods were also proposed. The above studies have demonstrated that the ULCC has obvious advantages, though the brittleness of the ULCC has limited its wider applications.

With the rapid development of the global economy and the automobile industry, the annual increase of waste tires over the world is currently about 8% to 10%. It is estimated that by 2020,

* Corresponding author. Tel: +86 755-86975402; Fax: +86 755-26732850; Emails: suill@szu.edu.cn; j.ye@lancaster.ac.uk

the output of waste tires in China will reach 20 million tons, which has become an emerging issue of environmental concerns. Traditional landfill and incineration not only cause huge environmental pollution, but also are energy inefficient. In 1996, Fedroff et al. [25] pioneered in producing rubberized concrete by mixing rubber powder made from grinding waste tires, which offered a new approach to recycle waste tires and started a new research topic on rubberized concrete. Many studies have since shown that, compared with the ordinary concrete, rubberized concrete has good resistance to crack and abrasion and energy dissipation capacity [26-34]. As an elastomer, rubber aggregates in concrete can restrain the generation and development of cracks, thus improve the energy dissipation capacities of concrete [25, 26]. However, adding rubber may reduce compressive strength, flexural strength and workability of concrete. To achieve improved energy dissipation, while still maintain sufficient material strength, adding additional mineral admixture such as silica fume and steel or polypropylene fibers are considered as commonly used and effective methods [27, 29, 37]. Nili et al. [28] conducted drop hammer impact tests on hooked steel fiber reinforced concrete with or without silica fume using the test method specified in ACI 544 [35]. The impact resistance of the concrete with 1% steel fiber and silica fume was twenty times higher than that of the plain concrete and 2.4 times higher than that of the concrete with silica fume only. Fiber-bridging plays a significant role in preventing crack and energy dissipating in the damage process. Similar findings were also concluded by Ali et al. [27] and Gupta et al. [29]. Guo et al. [37] reported that steel slag increased the stiffness and brittleness of the concrete in the static and SHPB impact tests. Yoo and Banthia [36] also studied the impact resistance of fiber reinforced concrete. Strain-rate sensitivities of fiber reinforced concretes depend on the types of loading and the strength of matrix. Tensile impacts are more sensitive to strain rate than compressive and flexural impacts are. Higher strength concrete is less sensitive compared to lower strength concrete. Liu et al. [30] evaluated the impact behavior of rubberized concrete of different rubber particle size and content through Splitting Hopkinson Pressure Bar (SHPB) tests. The results showed that with a fixed content of rubber, the dynamic compressive strength increased as the increase of the rubber particles size. However, when the rubber content exceeded 10% of the fine aggregate by weight, the energy dissipation capacity of the concrete started to decline.

The observations and conclusions made from the previous research have suggested that rubberized concrete is particularly beneficial to structures that require high impact resistance, such as high-rise buildings, long-span bridges, offshore platforms and other mega constructions. Moreover, these structures are normally very heavy due to their large cross sections that require more reinforcement. Thus, lightweight high strength concrete is a compromising alterative due to its unique advantages, such as low density, good thermal insulation and durability [13, 14]. Unfortunately, most of the existing lightweight concrete has low strength and is brittle, which has limited their applications. Hence, demands for new lightweight cement-based materials that have high ductility and good energy consumption are increasing. Naturally, using rubber aggregates to replace fine or coarse aggregates can reduce the weight and increase impact resistance, thus have the potential to meet the demand and recycle waste tires at the same time. To the authors' best knowledge, the research on the dynamic responses of rubberized LWAC is rare. The failure mechanism and strain rate sensitivity of the promising material also remain unclear.

This paper reports an experimental study on the development of an ultra-lightweight, high ductility cement composite with rubber powder and PE fibers. The mechanical properties of the new material, such as compressive strength, elastic modulus and damage modes under different strain rates are evaluated through static and SHPB impact tests. Furthermore, this paper proposes and validates a modified equation to predict the Dynamic Increasing Factor (DIF) of the new material.

2. Experimental Program

2.1 Materials and mix proportion design

To make the novel rubberized ultra-lightweight cement composite (RULCC) mixes, raw materials including cement, fly ash cenospheres (FAC), silica fume, rubber powder aggregate and PE fiber were used. The RULCC was designed to have a target 28-day compressive strength of around 35MPa with low density of around 1450kg/m^3. Fig. 1 shows the fine aggregates and their particle size distribution. The fine aggregate was FAC with a specific gravity of 870 kg/m^3, a fineness modulus of 0.902g/cm^3 and an average size of 20-300μm. The binder consisted of 100% of CEM I 52.5R ordinary Portland cement and 11 wt% of silica fume and 38.7-48.4wt% of FAC. The size of the rubber powder was 380μm, which was used to replace the FAC. A volume replacement of FAC with 5%, 10%, 15% and 20% rubber power were selected in the test. The water absorption of the rubber, which was surface treated, was less 1%. A picture of the rubber powder is shown in Fig. 1(b). To make a workable cement composite, a high-water reducing agent, polycarboxylate-based superplasticizer (SP) was used. The surface of the PE fibers was coated with hydrophilic. The mechanical properties of the PE fibers are shown in Table 2. The mix proportions are divided into seven groups as listed in Table 1, which includes mixtures with 5 different rubber replacement ratios (0%, 5%, 10%, 15% and 20% by volume of FAC), and 2 different fiber content (0% and 0.7% by volume).

Before casting, the slump flow of all the mixtures was measured based on ASTM C1611 as shown in Fig. 2. Good fluidity was maintained in all composites, but rubber particles had a negative effect on the fluidity of fresh ULCC. The specimens were demoulded after 24h curing at room temperature and were cured then in a standard fog room (temperature 20±2℃ and moisture ratio 95%) until the test day.

(a) Fly ash cenospheres (FAC)

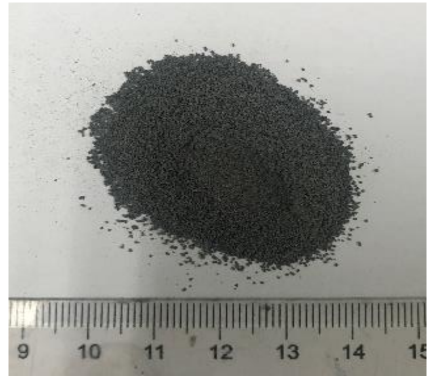

(b) Rubber powder

(c) Silica fume

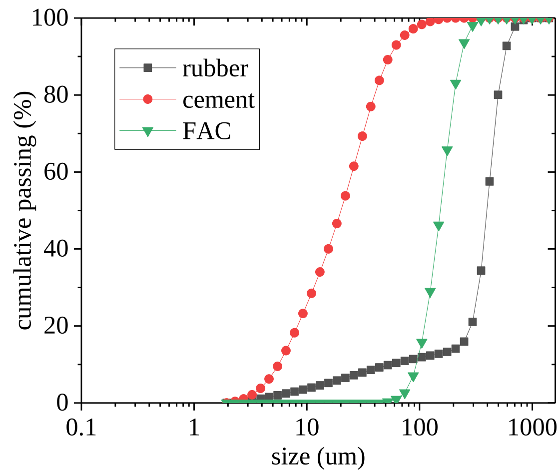

(d) Particle size distribution of raw materials

Figure 1 Fine aggregates and particle size distribution

Table 1 Mix proportions of RULCC (by weight)

Mix ID	Ce-ment	SF	FAC	Rubber	Water	SP	SRA	Fiber
R0-0	1	0.11	0.484	0.000	0.37	0.001	0.001	0
R5-0	1	0.11	0.460	0.027	0.37	0.001	0.001	0
R10-0	1	0.11	0.436	0.054	0.37	0.001	0.001	0
R15-0	1	0.11	0.412	0.080	0.37	0.001	0.001	0
R20-0	1	0.11	0.387	0.107	0.37	0.001	0.001	0
R0-0.7PE	1	0.11	0.484	0.000	0.37	0.001	0.001	0.7%
R10-0.7PE	1	0.11	0.436	0.054	0.37	0.001	0.001	0.7%

Note: SF=silica fume; FAC=fly ash cenospheres; SP= superplasticizer; SRA= shrinkage reducing agent. R10-0.7PE represents the RULCC with 10% rubber powder replacement of FAC and 0.7% PE fiber by volume.

Table 2 Mechanical properties of surface treated PE fiber

Diameter (μm)	Length (mm)	Density (g/cm^3)	Tensile strength (MPa)	Elastic modulus (GPa)	Fracture elongation (%)
24	12	0.97	3000	120	2-3

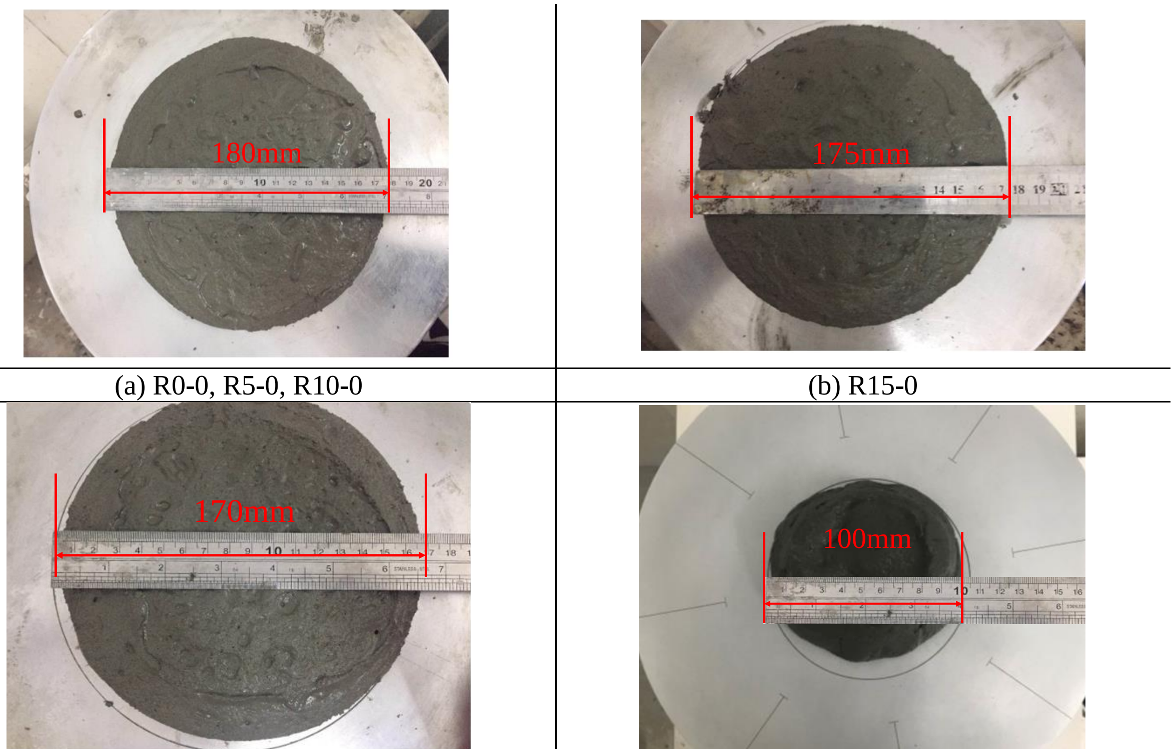

(a) R0-0, R5-0, R10-0
(b) R15-0
(e) R20-0
(f) R0-0.7PE, R10-0.7PE

Figure 2 Slump flow for typical RULCC

2.2 Test instrumentation and loadings

The static compression test was performed by using 300 tone MTS machine on a Φ100x200 cylinders, according to ASTM C39/C39M-01 (2014) [38]. Uniaxial static tensile test was carried out in accordance with the standard recommended by JSCE [39]. For each design mix, three concrete samples were prepared for the tests. Figure 3 shows the typical instrumentation for the compressive and tensile tests.

Scanning Electron Microscope (SEM) was conducted to observe the microscopic morphology of the RULCC using Quanta TM 250 FEG equipped with field emission environmental scanning mirror. The samples were taken from the central part of the broken pieces of the matrix without polishing process. Before scanning, the sample surfaces to be observed were gold coated and treated for conductivity.

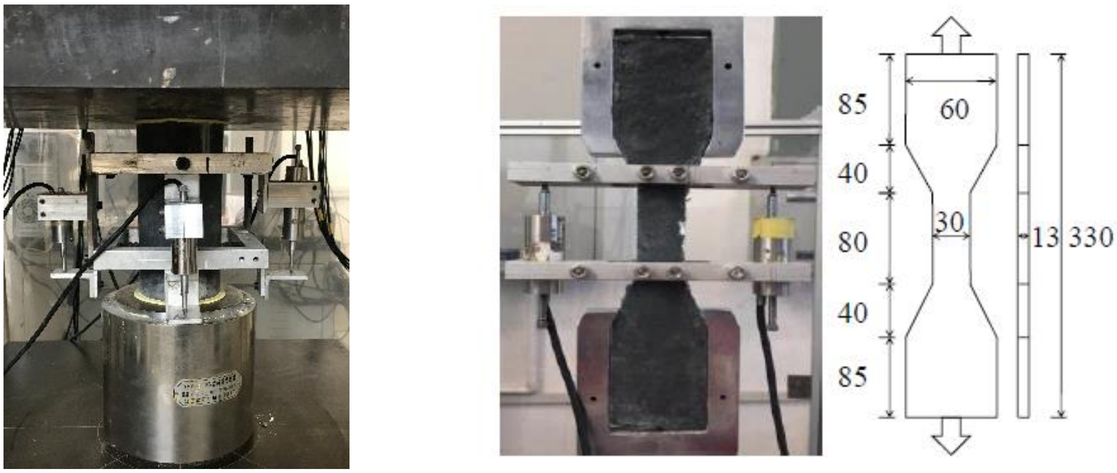

(a) Compressive test (b) Tensile test

Figure 3 Static test instrumentation for RULCC

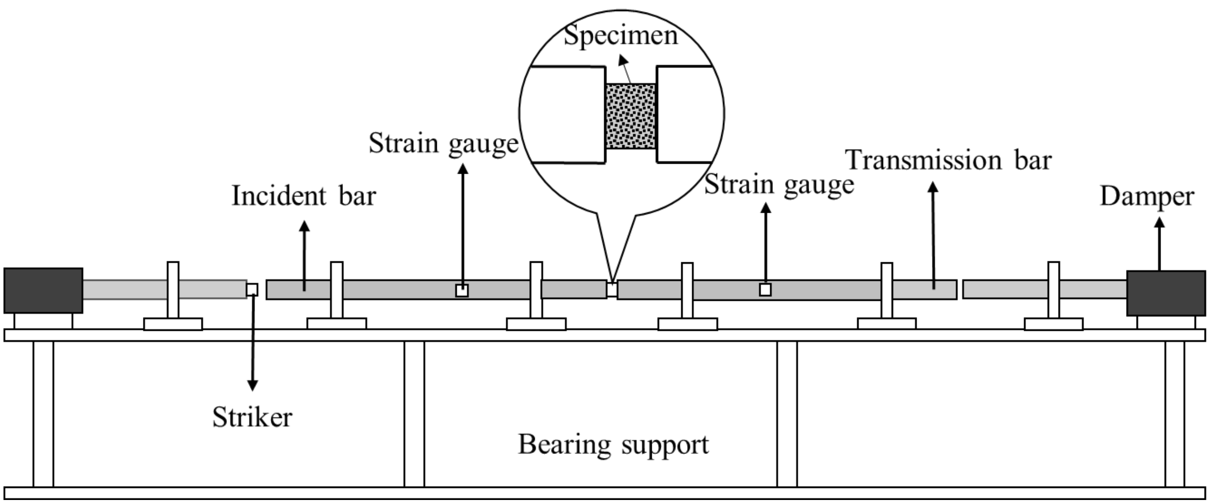

(a) Configuration of SHPB

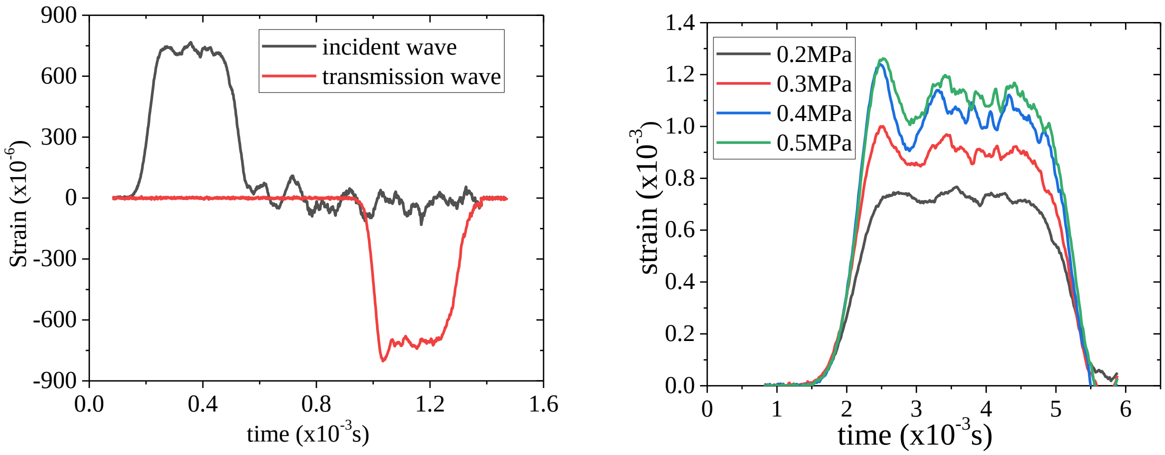

(b) Strain waveform for empty bar (c) Strain waveform under different pressure

Figure 4 SHPB test and impact waveform input

For the dynamic tests, SHPB tests were performed to investigate the dynamic behavior of the RULCC. For each strain rate, five concrete samples were tested, the results of which were averaged then to obtain the stress-strain curves, impact velocity, peak strain and peak stress, etc. SHPB test was first proposed by Hopkinson at the beginning of the last century [40]. The typical test configuration, consisting of a striker bar, an incident bar, a transmission bar, a damper and the specimen to be tested, is shown in Figure 4 (a). SHPB test is mainly based on the following two basic assumptions: (1) the stress pulse propagation is one-dimensional, and (2) the stress across the length of the specimen is uniform. Hypothesis (1) assumes that the strain measured by the strain gauge on the bar surface is identical to the strain on the end surface of the specimen, representing a uniform state of stress. Hypothesis (2) assumes that the effect of stress wave can be ignored, so that the specimen deforms uniformly under the uniform stress. The mechanical properties of the tested material can be characterized by the average stress and the average strain of the specimen obtained from the deformation of the bar. Figure 4(b) shows a classic waveform input. Based on the above two assumptions, the stress-strain relations of the specimens can be calculated by Eqs. (1)-(3),

$$\sigma = \frac{A_0}{A_s} E_0 \varepsilon_t(t) \tag{1}$$

$$\varepsilon = -2\frac{C_0}{L_s}\int_0^t \varepsilon_r(t)dt \tag{2}$$

$$\dot{\varepsilon} = -2\frac{C_0}{L_s}\varepsilon_r(t) \tag{3}$$

where, A_0 and A_s are, respectively, the cross section area of the bar and the specimen; E_0 and C_0 are the respective elastic modulus and elastic wave velocity of the rod; L_s is the length of the specimen; ε_t(t) and ε_r(t) are the transmission wave and the reflection wave in the bar, respectively. The impact rod of the SHPB used for the dynamic compressive test in this paper has a diameter of 120mm. The strain wave recorded from an empty test is shown in Figure 4(c) and the basic parameters of the SHPB for Eqs.(1-3) can be found in Table 3.

In order to control the flatness of the end surface of the specimens and reduce the friction effect of the contact surface between the bar and the concrete samples, a special grinding machine was used to prepare the concrete samples. The seven groups of specimens were subjected to four different strain rates relative to four different air pressures, i.e., 0.2MPa, 0.3MPa, 0.4MPa and 0.5MPa respectively. These pressures would induce the strain rates of 90/s to 190/s as mentioned in Section 3.3.3. The selected strain rates are the reprehensive rates of typical impacts, i.e., vehicle impact, ship impact and blast impact, which may occur to bridges, offshore platforms and military protective structures.

Table 3 Parameters for SHPB

A_0/(mm^2)	A_s/(mm^2)	E_0/(GPa)	C_0/(m/s)	L_s/(mm)
11309.7	7854.0	206	5100	50

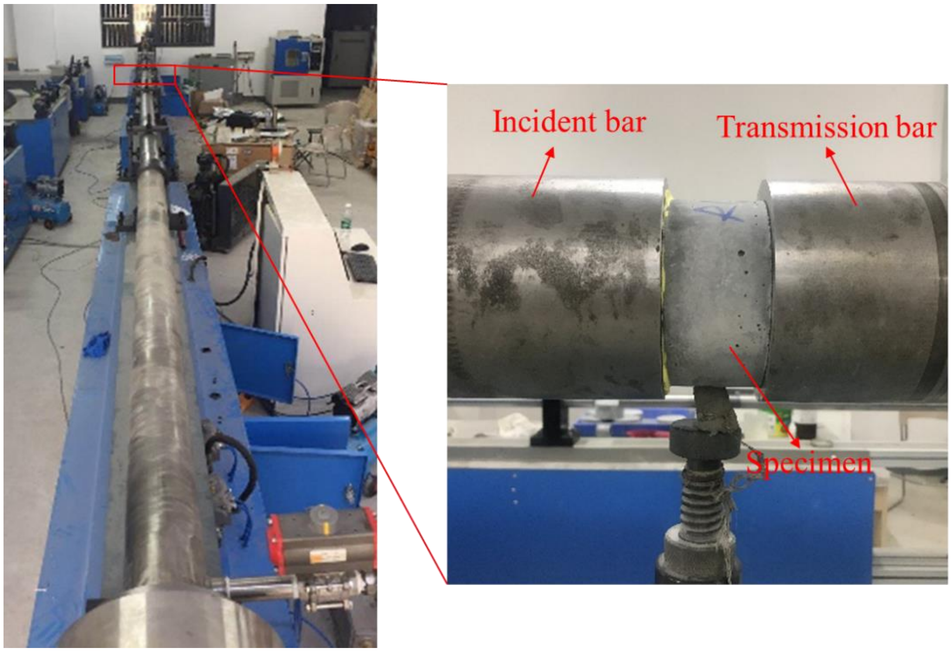

Figure 5 Split Hopkinson Pressure Bar and test sample

3. Test Results and Discussions

3.1 Static compressive test

The compressive strength of the RULCC decreases with the increase of rubber powder content. The compressive strength decreases by 29.5%, 47.7%, 54.8% and 60.3%, respectively, when 5%, 10%, 15% and 20% of the fine aggregates in the composites were replaced by rubber powder without fiber, as shown in Fig.6. As an organic polymer material, rubber powder has weak adhesion with cement based inorganic materials, resulting in a reduction of strength in the interfacial transition zone (ITZ). Each rubber particle distributed in the cement composites represent a weak spot that may initiate micro cracks and reduce compressive strength of the cement composites further. Similar finding was also reported by Liu et al. [30]. The elastic modulus of rubber is much lower than that of cement composite, leading to larger deformation of the rubber powder under quasi-static loading. The elastic modulus of the RULCC is much lower than that of normal concrete because of the lower elastic modulus of FAC and absence of coarse aggregates. It was found that the elastic modulus of the RULCC decreased by 15.7%, 29.3%, 32.1% and 33.6%, respectively, when 5%, 10%, 15% and 20% of the fine aggregates were replaced by rubber. Fig. 7(a) illustrates the morphology of the rubber powder and the FAC in the cracked composites using SEM. It is shown that the FACs are distributed uniformly in the cement composite, showing a good composite workability. There is no evidence of composite segregation in this test as reported in the previous tests that the lightweight FAC may float on the cement grout if segregation occurs [20]. Fig.7(b) is the image of a spalled composite with failure initiated from the ITZ between the rubber particles and the cement composite. The crack passed through this ITZ due to the weak bond strength. Without adding rubber powder, however, the specimen appeared to break and flake with a clear sound heard when it was crushed. Due to the larger deformation of rubber, the fragments of the specimens with rubber powder are larger than those from the specimens without added rubber. This observation indicates that the rubber powder reduces the brittleness of the ULCC. The addition of PE fibers to the R0-0 and R10-0 groups (R0-0.7PE and R10-0.7PE) reduces the compressive strength by 16.7% and 8.8%, respectively. This reduction may be attributed to that additional air bubbles are introduced during the mixing process as PE fibers are dispersed in the cement composites. Compared to the normal rubberized concrete [26], the RULCC has a greater reduction in compressive strength, mainly due to the following two factors: (1) Rubber aggregates are used to replace fine aggregate such as sand in normal concrete. However, in this test, the replacement ratio of rubber powder is proportional to the total aggregate volume, resulting in a larger replacement ratio than that of the normal rubberized concrete [29]; (2) The size of aggregate particles is normally within 0-10mm in normal concrete, which fills the pores to make the concrete more compact. However, the rubber powder has a maximum size of 380μm in this test, which is comparable to that of FAC (maximum size of 300μm), leading to less compact microstructure in the composite. In this case, cracks initiate from the ITZ that causes lower compressive strength. Future study should be conducted to investigate the effect of particle size of rubber powder.

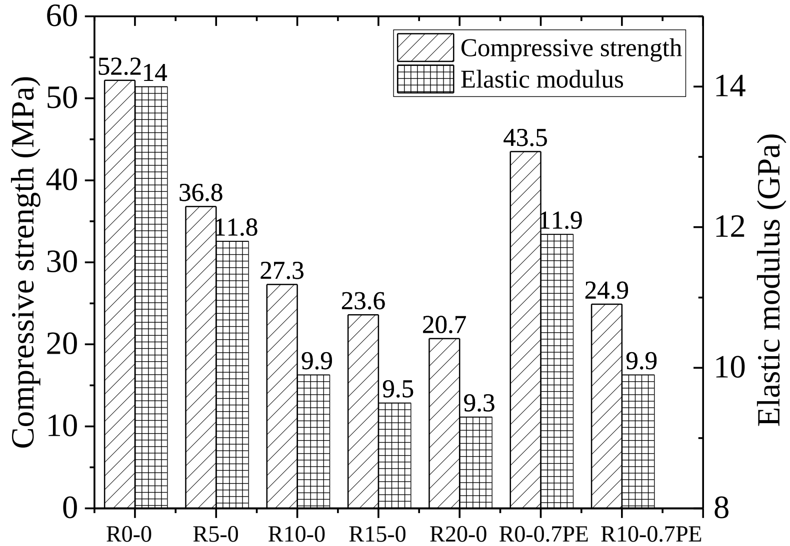

Figure 6 Compressive strength and elastic modulus of different RULCC mix

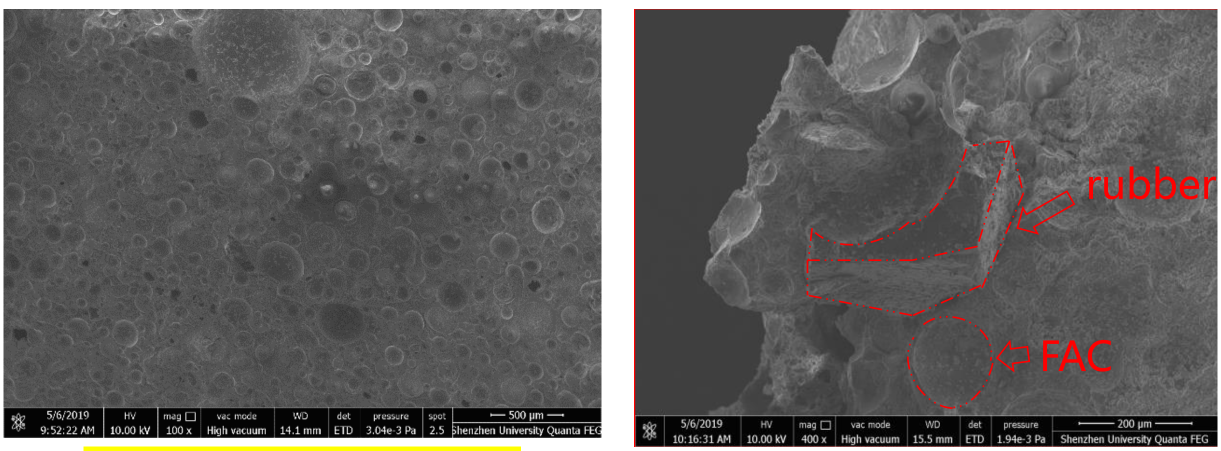

(a) Morphology of the composites

(b) Morphology of rubber powder and FAC in composites

Figure 7 SEM Morphology

3.2 Static tensile test

Figure 8 shows the direct tensile stress-strain curves of the RULCC coupon specimens. It is found that the tensile strain capacity of R0-0.7PE with low fiber content of 0.7% can reach 3%-4%, which is much higher than that of normal concrete, and meets the tensile strain requirements of the Engineered Cement Composite (ECC) materials [41]. The tensile strain capacity of R10-0.7PE with 10% rubber powder can reach about 4%-5%, showing promising ductile performance. Compared to the conventional ECC with 2% polymer fibers, RULCC can save 65% fiber content in volume, which shows great economic potentials for future applications. Figs. 8 and 9 illustrate the multiple micro cracking behavior of R0-0.7PE and R10-0.7PE, respectively. Based on the failure modes of R0-0.7PE and R10-0.7PE, the first crack appears when the stress reaches the tensile strength of the concrete substrate. The stress declines slightly but the load bearing capacity resumes very quickly due to the bridging effect of the PE fibers. This is followed by the next stage of local failure, leading to a progressive process that results in the formation of multiple fine cracks in the composites [4].

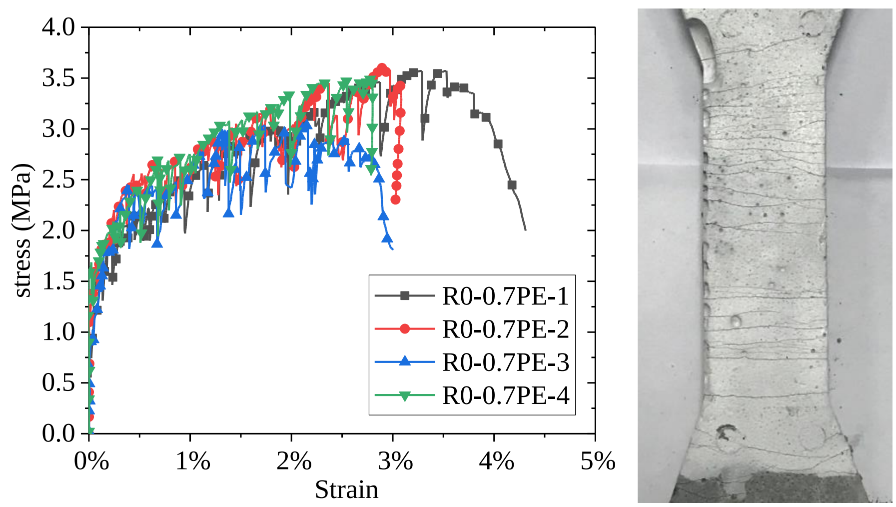

Figure 8 Tensile test of R0-0.7PE

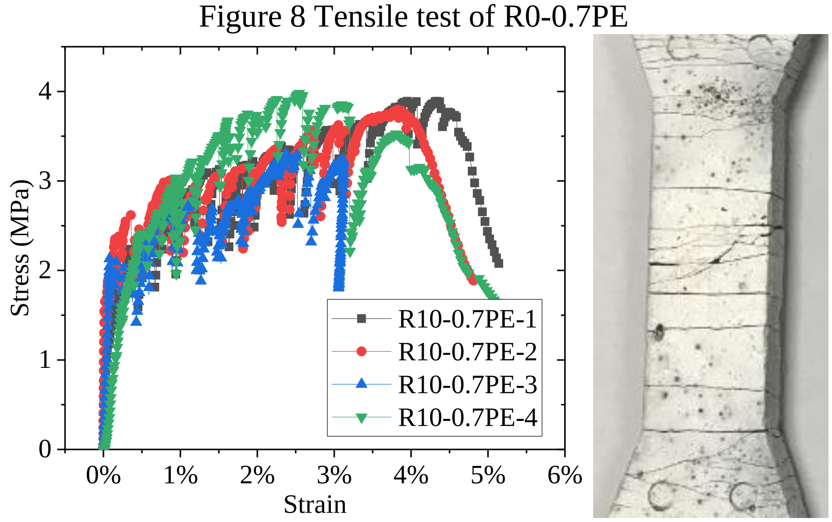

Figure 9 Tensile test of R10-0.7PE

3.3 Dynamic compressive test

3.3.1 Failure modes

The dynamic impact test on the RULCC was performed by the 120mm diameter SHPB. Fig.10 shows the failure modes of each mix group after the impact tests. Within a mix group, a higher strain rate causes more serious damage of the specimens. At the same strain rate, an increase of rubber content results in larger but less cement fragments, especially at a high strain rate, as shown in the comparisons between Figs. 10 (a)-(e). It should be noted that for the static compressive tests, because there are void defects in the composites, the damage is usually initiated from the weakest region to form a crack, leading to the final failure in the composite with only several main cracks. Unlike the static responses discussed previously, the rapid release of the impact energy under a high strain rate impact cannot be completed by the propagation of a single crack as the rate of crack opening is much slower. This delay leads to initiations of multiple cracks until the ultimate fragmentation occurs. After adding rubber powder into the cement composite, kinetic energy can be released more effectively due to the elastic deformation and energy dissipation capacity of rubber, thus reduce the number of the cracks with less fragmentation at failure. This observation is more obvious when more rubber is added. When PE fibers are introduced, the fibers tend to "tighten" the surrounding matrix during a low strain rate impact, thus only cracking without fragmentations are observed, as shown in Figs.10 (f) and (g). At a high strain rate of 146.8-185.1/s, the degree of damage of the rubberized mix group R10-0.7PE is similar to that of the non-rubberized group R0-0.7PE. All the specimens show both cracks and fragments and, hence, loss their integrity. The effect in preventing cracking of cement composite using low PE fiber content seems more pronounced than using rubber. However, the R5-0 group exhibits comparable energy dissipation capacity to R0-0.7PE, judged by the areas under the stress-strain curves shown in the next section.

0.2MPa (94.1/s) 0.3MPa (130.6/s) 0.4MPa (150.7/s) 0.5MPa (183.4/s)

(a) R0-0

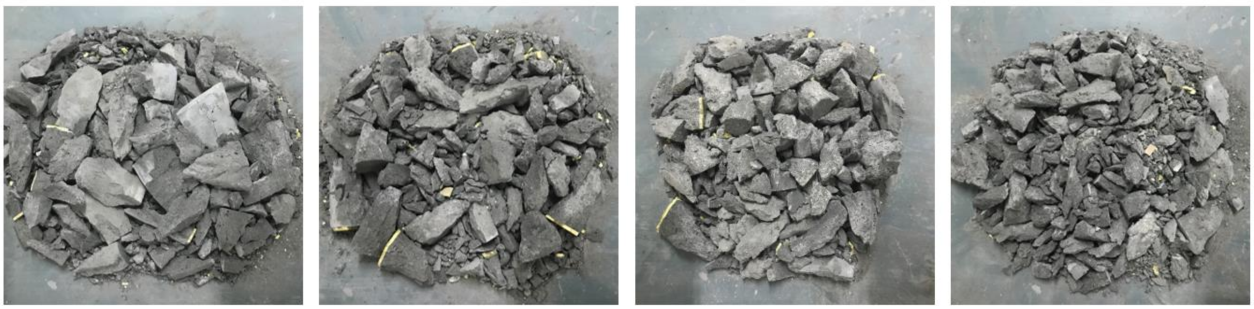

0.2MPa (91.9/s) 0.3MPa (123.4/s) 0.4MPa (149.9/s) 0.5MPa (178.6/s)

(b) R5-0

0.2MPa (105.3/s) 0.3MPa (128.4/s) 0.4MPa (155.7/s) 0.5MPa (181.5/s)

(c) R10-0

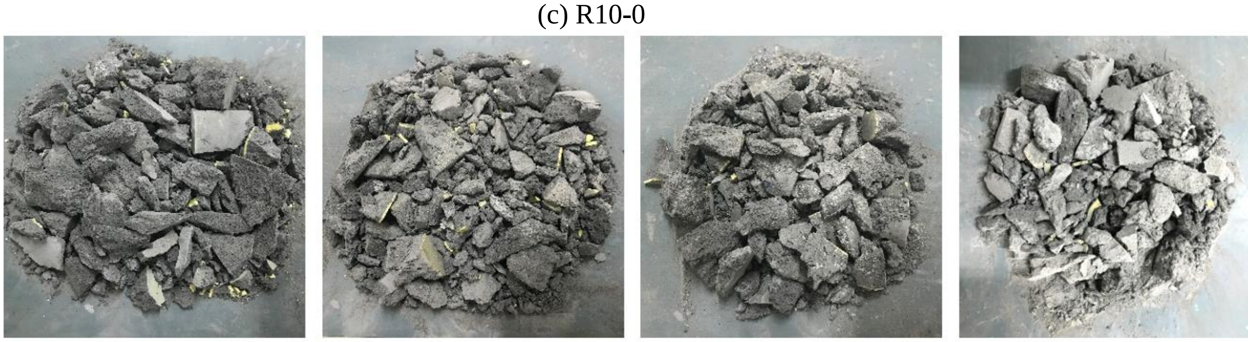

0.2MPa (104.8/s) 0.3MPa (129.2/s) 0.4MPa (159.8/s) 0.5MPa (180.9/s)

(d) R15-0

0.2MPa (99.7/s) 0.3MPa (123.5/s) 0.4MPa (150.5/s) 0.5MPa (186.5/s)

(e) R20-0

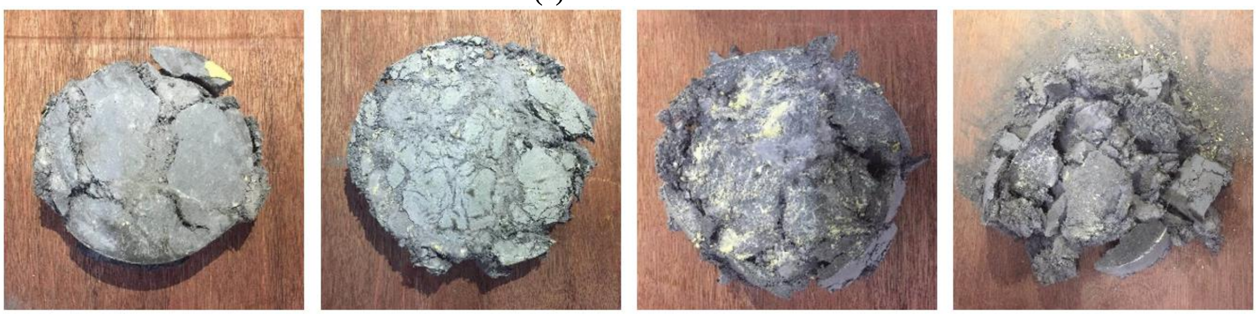

0.2MPa (102.1/s) 0.3MPa (128.3/s) 0.4MPa (146.8/s) 0.5MPa (166.4/s)

(f) R0-0.7PE

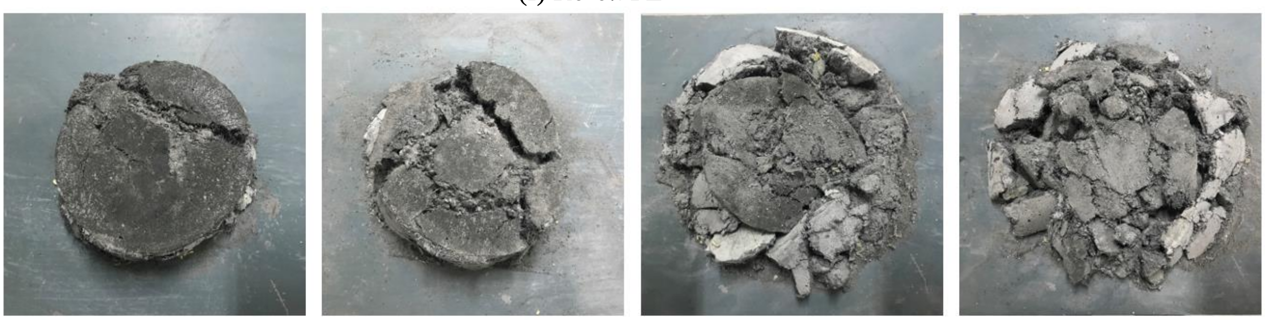

0.2MPa (93.1/s) 0.3MPa (138.2/s) 0.4MPa (158.7/s) 0.5MPa (185.1/s)

(g) R10-0.7PE

Figure 10 Failure modes of different mixture under different strain rate

3.3.2 Dynamic compressive stress-strain curves

Figure 11 shows the dynamic compressive stress-strain curves of the mix groups under different strain rates. Comparing Figs.11 (a) and (f), it is found that the stress-strain curves become smoother when PE fibers are added. Especially in the post-peak stress stage, the enclosed area under the stress-strain curves is increased, indicating that the addition of an appropriate amount of PE fibers can improve the dynamic strain capacity and enhance the ductility of the cement composites. This enhancement is similar to the effect of steel fiber on the concrete under impact loading as presented by Nili et al. [28]. Table 4 lists the dynamic peak strain and the enclosed area under the dynamic stress-strain curves of the concrete samples. It should be noted that the enclosed area is defined as the integration of the normalized peak stress ($\frac{\sigma_d}{\sigma_s}$) with regard to the strain. Comparing R5-0 with R-0-0.7PE in Table 4, it is found that energy absorption of the cement composite with 5% rubber powder and no fibers is comparable to that with 0.7% PE fibers and no rubber. During the impact process, the rubber particles tend to dissipate impact energy due to the large peak strain when the crack propagates to the rubber particles, leading to enhanced deformation capacity of the RULCC and, thus, reduced size of the fragments at failure. Comparing R0-0 with R5-0, the enclosed area under the stress-strain curves increases by 49.6%, 78.0%, 76.9% and 39.2%, respectively, for the varying strain rates, and the dynamic peak strain increases by 189%, 246% and 19%, respectively, when the load pressure increases from 0.3MPa to 0.5MPa. Compared with the R0-0 group, the added rubber results in an increase in peak stress. The average ratios of the increase are 92.5%, 71.6%, 81.3% and 85.8%, respectively, when 5%, 10%, 10% and 15% and 20% rubber are added, which demonstrates that the peak stress of the composites with rubber is more sensitive to the strain rate compared to those without rubber. However, as the rubber content exceeded 10% of the FAC by weight, the enclosed area seems to reduce, indicating that the energy dissipation capacity of the RULCC started to decline. This also matches the test results reported by Liu et al. [30]. Comparing R0-0 with R0-0.7PE, the addition of PE fibers increases the enclosed area by 22.3%, 23.4%, 66.0% and 42.1%, respectively as the strain rate takes 102.1/s, 128.3/s, 146.8/s and 166.4/s, which shows that adding PE fibers also has significant effect on energy dissipation. However, when fibers are added into R10-0, the enclosed area is reduced considerably compared to R0-0.7PE. It may be mainly due to the poor bonding strength of the ITZ between the fibers and the cement composite when a significant amount (10%) of rubber powder are added. Based on the analysis of the enclosed area in the dynamic stress-strain curves, a rubber replacement ratio of 5%-10% seems to be an appropriate ratio for the RULCC in terms of energy dissipation capacity.

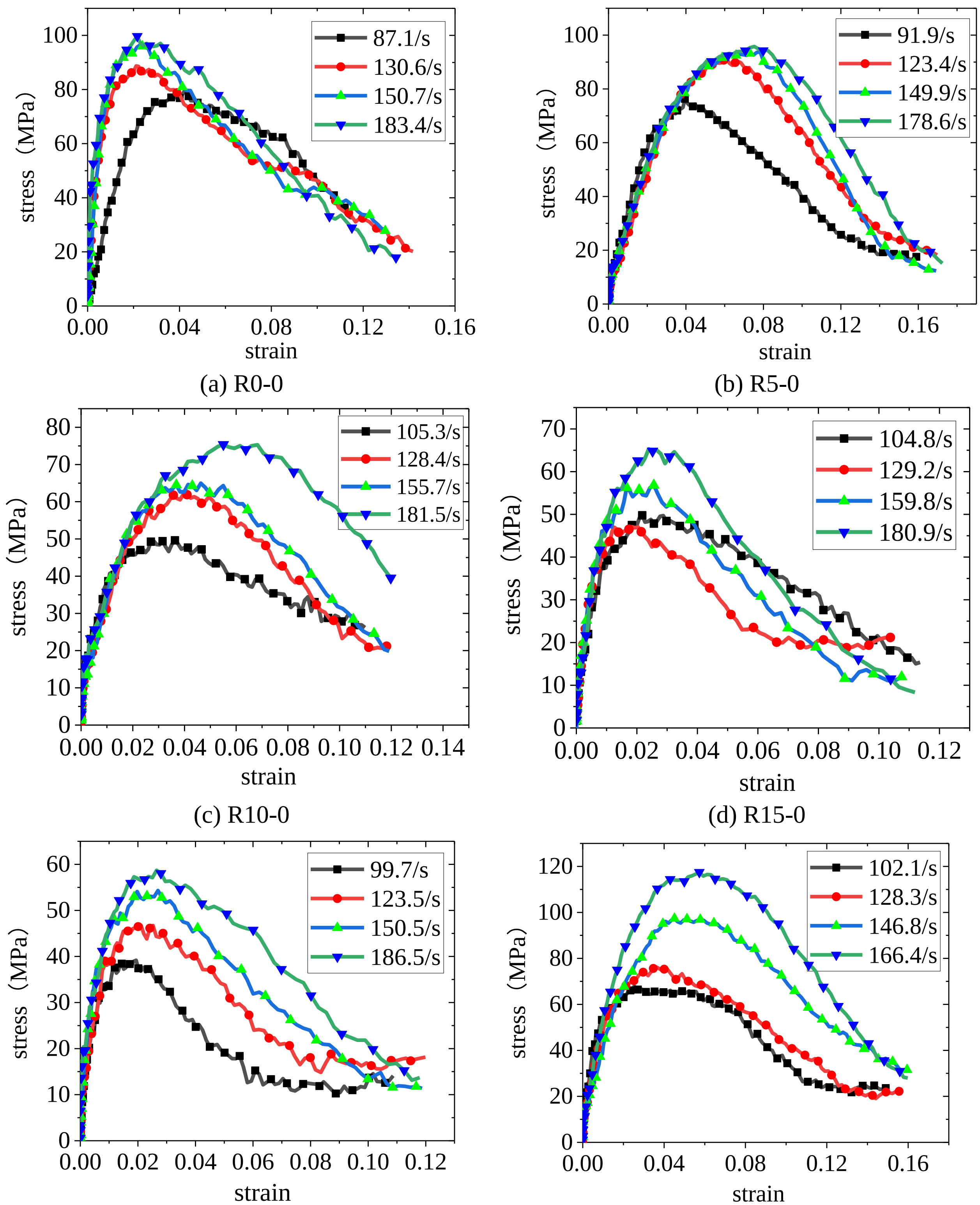

(e) R20-0

(f) R0-0.7PE

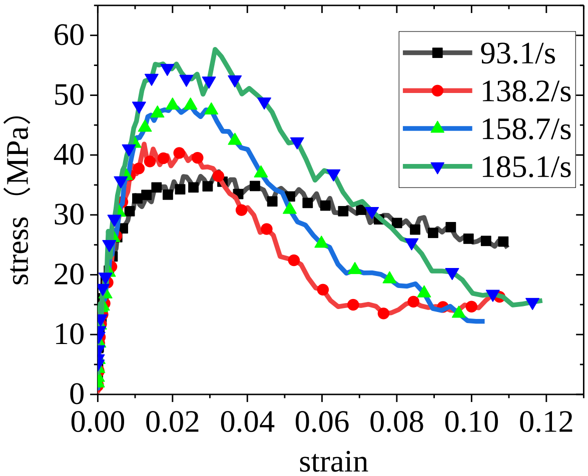

(g) R10-0.7PE

Figure 11 Dynamic compressive stress-strain curves

Table 4 SHPB test results

MIX ID	Static compressive strength (MPa)	Impact velocity (m/s)	Strain rate (/s)	Dynamic peak stress (MPa)	Dynamic peak strain	Enclosed area of stress-strain curve
R0-0	52.2	8.3	94.1	79.7(52.7%*)	4.298%(8.6#)	1.29
		10.3	130.6	88.7(69.9%)	2.112%(3.7)	1.41
		12.3	150.7	96.4(84.7%)	2.267%(4.0)	1.47
		13.0	183.4	100.8(93.1%)	6.320%(13.0)	2.09
R0-0.7PE	43.5	8.7	102.1	68.0(56.3%)	2.527%(4.6)	1.58
		10.9	128.3	76.3(75.4%)	3.601%(7.0)	1.74
		12.5	146.8	97.3(123.7%)	4.510%(9.0)	2.44
		14.0	166.4	117.5(170.1%)	5.734%(11.7)	2.97
R5-0	36.8	8.4	91.9	76.3(107.3%)	3.948%(7.8)	1.93
		10.5	123.4	91.2(147.8%)	6.104%(12.6)	2.51
		12.2	149.9	93.7(154.6%)	7.838%(16.4)	2.60
		13.6	178.6	95.8(160.3%)	7.527%(15.7)	2.91
R10-0	27.3	8.2	105.3	49.6(81.7%)	3.633%(7.1)	1.52
		10.7	128.4	62.1(127.5%)	3.964%(7.8)	1.84
		12.0	155.7	65.0(138.1%)	4.631%(9.3)	2.01
		13.7	181.5	74.6(173.3%)	5.506%(11.2)	3.05
R10-0.7PE	24.9	8.7	93.1	37.4(50.2%)	3.236%(6.2)	1.35
		10.7	138.2	41.9(68.3%)	1.242%(1.8)	1.03
		12.4	158.7	48.3(94.0%)	2.002%(3.4)	1.23
		13.8	185.1	57.6(131.3%)	3.140%(6.0)	1.67
R15-0	23.6	8.5	104.8	49.4(109.3%)	2.644%(4.9)	1.70
		10.6	129.2	50.3(113.1%)	4.567%(9.1)	1.76
		12.3	159.8	56.8(140.7%)	2.561%(4.7)	1.35
		13.6	180.9	65.3(176.7%)	2.391%(4.3)	1.70

R20-0	20.7	8.0	99.7	40.8(97.1%)	1.938%(3.3)	1.08
		10.4	123.5	46.8(126.1%)	2.107%(3.7)	1.60
		12.1	150.5	53.7(159.4%)	2.696%(5.0)	1.83
		13.6	186.5	57.4(177.3%)	2.650%(4.9)	2.18

*, #:the value in the bracket represents the increasement ratio compared to the static value.

3.3.3 Effect of strain rate

Figure 12 shows the relationships between the strain rate and the dynamic increasing factor (DIF) for normal concrete, conventional rubberized concrete, ULCC and the RULCC subjected to dynamic load. It is evident that the RULCC is more sensitive to the strain-rate on the dynamic compressive strength compared to the normal concrete, normal rubberized concrete and ultra-lightweight concrete. Similar to the observations from the previous investigations [26, 30, 31], the strength of concrete increases with the increase of strain rate. In this paper, different load pressure (0.2MPa, 0.3MPa, 0.4MPa and 0.5MPa) with respective strain rates of 91.9~105.3/s, 123.4~138.2/s, 149.9~159.8/s, 166.4~186.5/s are considered. By plotting the relationship between the DIF and strain rate in Fig 13, it can be found that with the increase of strain rate, DIF increases approximately linearly with the strain rate. The reason for this is mainly due to the different failure modes and the loading period of the RULCC under different strain rates. The static compression failure originates from micro-cracks in the weak regions and propagation of them to form one or several major cracks, while the dynamic compression failure is due to a large number of micro-cracks generated simultaneously. In principle, the development of concrete cracks can consume a large amount of energy, especially with a high strain rate. A higher velocity impact always generates more micro-cracks that consume more energy. In the process of dynamic compression failure, the formation and propagation of cracks require significant energy. Generally, a higher loading rate inevitably leaves less time for the material to consume energy through generating and developing cracks, or store energy through deformation. Thus, an increase of stress is obvious due to the strain-rate effect.

Figure 13(a) shows the effect of strain rate on the dynamic compressive strength of the RULCC. For the strain rate of 91.9-186.5/s, the dynamic compressive strength of all the mixes increase approximately linearly as the strain rate increases. However, the strength of R0-0.7PE increases significantly when the strain rate is greater than 146.8/s. This indicates that the PE fiber may have significant effect on the gain in dynamic compressive strength since cracks in the composites may interact with inclined fibers that often lead to fiber bridging and improved fracture resistance. Composites with flexible PE fibers may undergo strain hardening and absorb more impact energy in the loading process, while this effect is not pronounced for other RULCC groups with rubber powder.

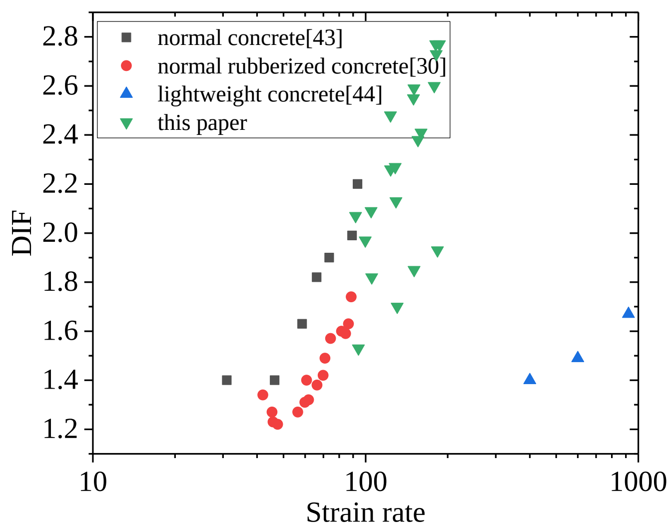

Figure 12. DIF of different types of concrete

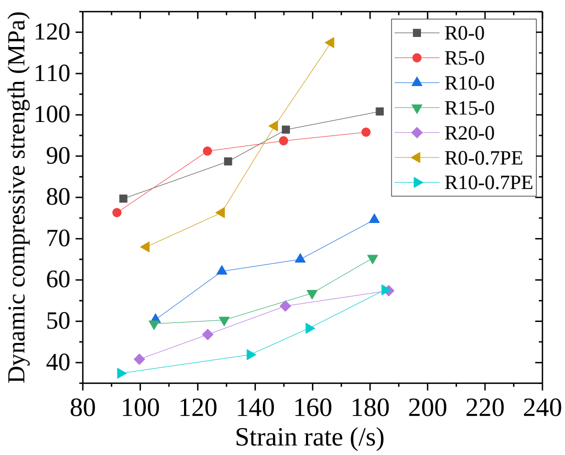

(a) Compressive strength under varying strain rates

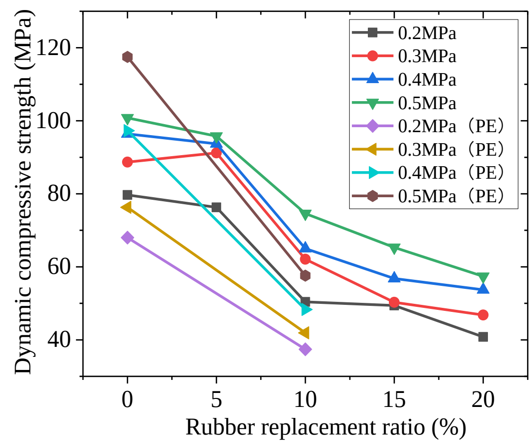

(b) Compressive strength with different amount of rubber powder

Figure 13. Effect of strain rate and rubber replacement ratio

3.3.4 Effect of rubber content

Figure 13 (b) shows the relation between the dynamic compressive strength and the amount of rubber in the composites. Basically, the dynamic compressive strength decreases considerably as the rubber content increases, which is similar to the observation when the materials are subjected to static compression. This is mainly because rubber is hydrophobic, has poor bond strength to the cement composite and low elastic modulus. For the RULCC groups with and without PE fibers, the dynamic compressive strength deceases with increase of rubber replacement ratio.

4. Analytical Modeling

4.1 Modified equation for DIF

DIF is an indicator of strength improvement that is defined as the ratio of dynamic compressive strength to static compressive strength [26, 29-31]. CEB-FIP [8] proposed a formula to calculate the DIF of normal concrete with respect to the strain rate. Chen [26] also proposed a formula to calculate the DIF for the conventional rubberized concrete while Ngo et al. [42] proposed a formula to predict the DIF for the high strength concrete. The abovementioned formulas are summarized in Table 5.

Table 5 Existing DIF model in the references

References	Concrete type	DIF formulae
CEB-FIP [8]	Normal concrete	$DIF=\frac{\sigma_d}{\sigma_s}=\begin{cases}\left(\frac{\dot{\varepsilon}_c}{\dot{\varepsilon}_s}\right)^{0.014} & \dot{\varepsilon}_d \le 30\mathrm{s}^{-1}\\ 0.012\left(\frac{\dot{\varepsilon}_c}{\dot{\varepsilon}_s}\right)^{\frac{1}{3}} & \dot{\varepsilon}_d > 30\mathrm{s}^{-1}\end{cases}$
Chen [26]	Conventional rubberized concrete	$DIF=\frac{\sigma_d}{\sigma_s}=0.9079\left(\dot{\varepsilon}_d\right)^{0.3158}\gamma \quad \dot{\varepsilon}_d > 30s^{-1}$ $\log\gamma = 6.156\alpha - 0.492$ $\alpha=\left(5+3\left(101.6-1.85R\right)\% f_{cu}/4\right)^{-1}$
Ngo et al. [42]	High strength concrete	$DIF=\frac{\sigma_d}{\sigma_s}=\left(\frac{\dot{\varepsilon}_d}{\dot{\varepsilon}_s}\right)^{1.026\alpha} \quad \dot{\varepsilon}_c \le \dot{\varepsilon}_1$ $DIF=\frac{\sigma_d}{\sigma_s}=A\times\ln\dot{\varepsilon}_d - B \quad \dot{\varepsilon}_c > \dot{\varepsilon}_1$ $A=-0.0044\sigma_s+0.9866$, $B=-0.0128\sigma_s+2.1396$ $\alpha=1/(20+\sigma_s)/2$, $\dot{\varepsilon}_1=0.0022\sigma_s^{\ 2}-0.1989\sigma_s+46.137$

* σ_d and σ_s denote dynamic and static compressive strength, respectively; $\dot{\varepsilon}_d$ and $\dot{\varepsilon}_s$ are the respective dynamic and static strain rates; f_{cu} is the compressive strength of concrete in MPa; *R* is the rubber content by volume fraction.

Table 6 gives the predictions of DIF calculated by CEB-FIP [8], Chen's model [26] and Ngo et al.'s model [42] for the RULCC developed in this paper. Obviously, CEB-FIP model overestimates the DIFs when comparing to the test results of the composites without rubber aggregates. Because of the similar brittleness behavior of the high strength and the lightweight concrete, the DIFs predicted by Ngo et al.'s model are close to the test results of R0-0 when no rubber is added to the ULCC. With added rubber, however, the predictions are less accurate. Generally speaking, Chen's model may give scattered predictions of DIFs for the RULCC of this paper since the model was proposed for normal rubberized concrete. By introducing rubber volume to the formula as a parameter, for the low content rubber (R5-0), Chen's model underestimates the DIFs. However, for the high content rubber (R10-0, R15-0 and R20-0), Chen's model overestimates the DIFs. On the basis of the above work and the test results, modified DIF equations are proposed in this paper for ULCC and RULCC, respectively.

For ULCC matrix, the new DIF formula follows the structure of the CEB-FIP's equation, i.e.,

$$DIF = \frac{\sigma_d}{\sigma_s} = 0.0106\left(\frac{\dot{\varepsilon}_c}{\dot{\varepsilon}_s}\right)^{\frac{1}{3}} \qquad \dot{\varepsilon}_d > 30s^{-1} \tag{4}$$

For rubberized ultra-lightweight cement composites, DIF takes the form as proposed by Ngo et al. [42], considerring that the behaviour of ultra-lightweight cement composites is similar to that of high strength concrete. It should be noted that β and γ are considered as functions of the rubber replacement ratio R, so that the effect of the ratio can be properly included in the formula. This is different from the CEB-FIP equation that can not consider the rubber content. In Chen's model, the compressive strength and R are both included in the formula. Althought the formula can consider the effect of the rubber replacement ratio and matrix strength through a rather complex calculation process, the dimensions of the formula are not consistance, which may require further revaluation. Considering of abovementioned factors and take advantages of the tests results of this study, a modified DIF formula is proposed below.

$$DIF = \frac{\sigma_d}{\sigma_s} = \beta \times \lg\left(\frac{\dot{\varepsilon}_c}{\dot{\varepsilon}_s}\right) - \gamma \qquad \dot{\varepsilon}_d > 30s^{-1} \tag{5}$$

where, β and γ are defined as a linear function of rubber replacement ratio R in volume fraction, i.e., $\beta = 8.121R + 1.458$, $\gamma = 54.587R + 7.250$, where the constants are obtained from the experimental results through regression. The DIF of RULCC calculated from Eq.(5) is larger than that of normal concrete, which indicates that RULCC is more sensitive to strain rate. ULCC has more air bubbles and smaller elastic modulus, leading to a higher deformation capacity and energy absorption performance.

4.2 Verification of the proposed model

Table 6 presents the DIFs calculated by the CEB-FIP model (DIF_{CEB}), Chen's model ($DIF_{[26]}$), Ngo et al.'s model ($DIF_{[42]}$) and the newly proposed model (DIF_{pre}) in this paper. From the table, it is shown that the average values of DIF_{test}/DIF_{CEB}, $DIF_{test}/DIF_{[21]}$, $DIF_{test}/DIF_{[40]}$, DIF_{test}/DIF_{pre} are 1.12, 0.96, 1.22 and 0.99, respectively, with standard deviations of 0.14, 0.11, 0.16 and 0.05. It can also be seen that using of CEB-FIP and Ngo et al.'s model directly may underestimate the DIFs for the ULCC and the RULCC. The newly proposed model provides better prediction to the DIFs with the smallest standard deviations for both the ULCC and the RULCC. Chen's model gives reasonably accurate predictions for the ULCC without added rubber, but with slightly larger deviation. Fig.14 plots and compares the DIF curves using all the above models for the ULCC and the RULCC groups. It should be noted that the newly proposed DIF formula is a function of the strain rate and the rubber replacement ratio *R*, which is different from the CEB-FIP prediction that takes exponential function for all types of concrete when the strain rate is beyond $30s^{-1}$. It can be seen from the comparisons that all the experimental results fall within the two curves predicted by the newly proposed model. To further verify the propose model, further new independent impact tests on the RULCC with different rubber replacement ratios arranged from 0% to 20% were conducted. Figure 14 also compares the formulas with the additional independent test data in the DIF-strain rate curves, which again demonstrates that the proposed DIF model can provide accurate predictions and potentially be used in dynamic design of RULCC in the future.

Table 6 Verification of DIFs by the existing models

MIX ID	σ_s (MPa)	σ_d (MPa)	DIF_{test}	DIF_{CEB}	DIF_{test}/DIF_{CEB}	$DIF_{[26]}$	$DIF_{test}/DIF_{[26]}$	$DIF_{[42]}$	$DIF_{test}/DIF_{[42]}$	DIF_{pre}	DIF_{test}/DIF_{pre}
R0-0	52.2	79.7	1.53	1.76	0.87	1.69	0.91	1.64	0.93	1.55	0.99
		88.7	1.70	1.96	0.87	1.87	0.91	1.81	0.94	1.73	0.98
		96.4	1.85	2.06	0.90	1.96	0.94	1.89	0.98	1.82	1.02
		100.8	1.93	2.19	0.88	2.08	0.93	2.00	0.97	1.94	0.99
R5-0	36.8	76.3	2.07	1.74	1.19	1.87	1.11	1.63	1.27	2.11	0.98
		91.2	2.48	1.92	1.29	2.06	1.20	1.78	1.39	2.35	1.06
		93.7	2.55	2.05	1.24	2.19	1.16	1.88	1.36	2.51	1.02
		95.8	2.60	2.17	1.20	2.31	1.13	1.98	1.31	2.65	0.98
R10-0	27.3	49.6	1.82	1.82	1.00	2.21	0.82	1.70	1.07	2.15	0.85
		62.1	2.27	1.95	1.16	2.35	0.97	1.80	1.26	2.34	0.97
		65.0	2.38	2.08	1.14	2.50	0.95	1.90	1.25	2.54	0.94
		74.6	2.73	2.19	1.25	2.62	1.04	1.99	1.37	2.69	1.01
R15-0	23.6	49.4	2.09	1.82	1.15	2.36	0.89	1.69	1.24	2.07	1.01
		50.3	2.13	1.95	1.09	2.52	0.85	1.80	1.18	2.32	0.92
		56.8	2.41	2.10	1.15	2.69	0.90	1.92	1.26	2.56	0.94
		65.3	2.77	2.18	1.27	2.80	0.99	1.99	1.39	2.71	1.02
R20-0	20.7	40.8	1.97	1.79	1.10	2.48	0.79	1.67	1.18	1.93	1.02
		46.8	2.26	1.92	1.18	2.65	0.85	1.78	1.27	2.22	1.02
		53.7	2.59	2.05	1.26	2.82	0.92	1.89	1.37	2.48	1.04
		57.4	2.77	2.21	1.25	3.02	0.92	2.01	1.38	2.77	1.00
Mean.					1.12		0.96		1.22		0.99
Std.					0.14		0.11		0.16		0.05

* Corresponding author. Tel: +86 755-86975402; Fax: +86 755-26732850; Emails: suill@szu.edu.cn; j.ye@lancaster.ac.uk

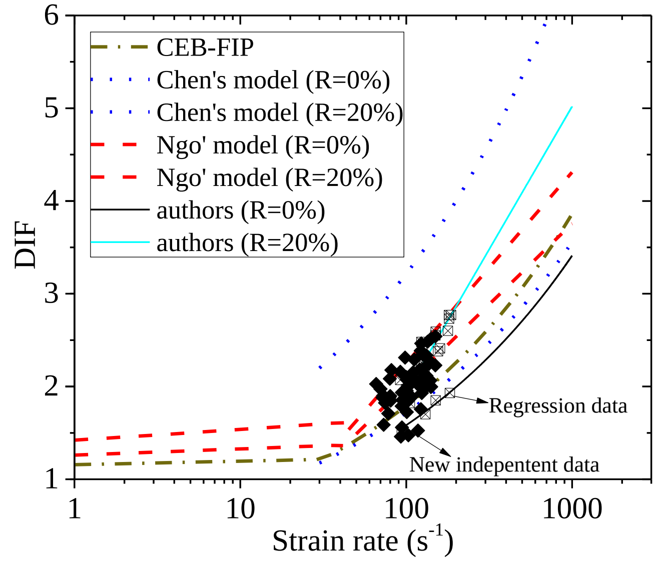

Figure.14 Proposed DIF model v.s. existing DIF models

5. Conclusions

This paper develops a novel ultra-lightweight high ductility cement composite (RULCC) with added low content of PE fibers (0.7%) and different amount of rubber powder. The paper investigates the dynamic behavior of the RULCC based on the Split Hopkinson Pressure Bar tests and proposes modified equations to predict the Dynamic Increasing Factor (DIF) of the material. The following conclusions have been made on the basis of this study.

(1) The novel rubberized ultra-lightweight cement composite (RULCC) has a low density of 1450kg/m^3 with high compressive strength of 52.2MPa. The RULCC incorporated with low PE fiber content 0.7% (R0-0.7PE) exhibits 3%-4% tensile strain capacity, while that with another 10% added rubber powder (R10-0.7PE) could still have a strength of 24.9MPa, but an increase of tensile strain up to 4-5%, showing its high ductility performance. Multiple micro cracking behavior can be achieved in the RULCC. Compared to the conventional Engineering Cementitious Concrete (ECC) with 2% polymer fibers, RULCC can save 65% fiber content in volume which could be an economic solution for future applications.

(2) The static compressive strength of the RULCC decreases with the increase of rubber powder content. The reduction in the strength are the results of the lower elastic modulus of the rubber powder and the weak bond strength between the rubber particles and cement composite. The elastic modulus of the RULCC is much lower than that of normal concrete because of lower elastic modulus of FAC and absent of coarse aggregates.

* Corresponding author. Tel: +86 755-86975402; Fax: +86 755-26732850; Emails: suill@szu.edu.cn; j.ye@lancaster.ac.uk

(3) The SHPB compressive test shows that the rubber powder particle (less than 10% in volume) can improve the impact resistance of ULCC. The dynamic compressive strength decrease gradually as the rubber content in the composites increases. Compared to the materials without added rubber, the specimens exhibit better energy absorption performance. The enclosed areas in stress-strain curves of the RULCC groups increase significantly. Low content PE fiber (0.7%) in cement composite can maintain integrity of the concrete and considerably increase the DIFs, due to the bridging effect of PE fiber. RULCC is more sensitive to strain rate, compared to normal concrete, lightweight aggregate concrete and high strength concrete.

(4) This paper proposes an effective model considering the strain rate effects and rubber replacement ratio R to predict the DIFs. The proposed model provides improved predictions of DIFs for ULCC and RULCC, when compared to CEB-FIP, Chen's and Ngo et al.'s model. The newly proposed equations can be used to predict the DIFs of the novel RULCC subjected to impact.

Acknowledgement

The authors would like to acknowledge the research grant received from the National Natural Science Foundation of China (NSFC, No.51708360, 51978407), Innovative Project Funded by Ministry of Guangdong Province Education Office (No.2017KTSCX164), Shenzhen Basic Research Project (NO. JCYJ20180305124106675). The authors also would like to acknowledge Professor Liu Laibao from Xinan University of Technology for providing the rubber powder materials and Professor Dong Zhijun for providing SHPB test facility.

References

[1] Yingwu Zhou, Xiaoming Liu, Feng Xing, Hongzhi Cui, Lili Sui; Axial compressive behavior of FRP-confined lightweight aggregate concrete: An experimental study and stress-strain relation model, Construction and Building Materials, Vol. 119, 1-15, 2016.

[2] Tommy Yiu Lo, Hongzhi Cui, Shazim Ali Memon, Takafumi Noguchi, Manufacturing of sintered lightweight aggregate using high-carbon fly ash and its effect on the mechanical properties and microstructure of concrete, Journal of Cleaner Production, Vol. 112, 1, 753-762, 2016.

[3] Zhenyu Huang, Krishnan Padmaja, Shan Li, J.Y. Richard Liew, Mechanical properties and microstructure of ultra-lightweight cement composites with fly ash cenospheres after exposure to high temperatures, Construction and Building Materials,2018;164:760-774.

[4] Z.Y. Huang, F. Wang, Y.W. Zhou, L.L. Sui, P. Krishnan, J.Y.R. Liew, A novel, multifunctional, floatable, lightweight cement composite: development and properties, Mater. 11 (10) (2018) 2043-2062.

[5] Derek Kramar, Vivek Bindiganavile, Impact response of lightweight mortars containing expanded perlite, Cem. Concr. Compos. 37 (2013) 205–214.

[6] Remzi Sahin, Ramazan Demirbog˘a, Habib Uysal, Rüstem Gül, The effects of different cement dosages, slumps and pumice aggregate ratios on the compressive strength and densities of concrete, Cem. Concr. Res. 33 (8) (2003) 1245–1249.

[7] JGJ 51-02. Technical specification for lightweight aggregate concrete. Beijing: China Academy of Building Research; 2002.

[8] CEB. CEB-FIP Model Code 2010-First Complete Draft, vol. 1. Lausanne, Switzerland. Committee Euro-International du Beton; 2010.

[9] BS, EN 13055. Lightweight aggregates, in part 1: Lightweight aggregates, Lightweight aggregates for concrete, mortar and grout. London: British Standards Institution; 2016.

[10] ASTM, C 213R-14. Guide for structural lightweight aggregate concrete. West Conshohocken (PA): ASTM International; 2014.

[11] ASTM, C 330-17. Standard specification for lightweight aggregates for structural concrete. West Conshohocken (PA): ASTM International; 2017.

[12] H.Z. Cui, T.Y. Lo, S.A. Memon, F. Xing, X. Shi, Analytical model for compressive strength, elastic modulus and peak strain of structural lightweight aggregate concrete, Constr. Build. Mater. 36 (2012) 1036-1043.

[13] M.H. Zhang, O.E. Gjorv, Mechanical properties of high-strength lightweight concrete, ACI Mater. J. 88 (3) (1991) 240-247.

[14] Z.Y. Huang, J.Y.R. Liew, W. Li, Evaluation of compressive behavior of ultra-lightweight cement composite after elevated temperature exposure, Constr. Build. Mater. 148 (2017) 579-589.

[15] Z.Y. Huang, J.Y.R. Liew, Nonlinear finite element modelling and parametric study of curved steel–concrete–steel double skin composite panels infilled with ultra-lightweight cement composite, Constr. Build. Mater. 95 (2015) 922-938.

[16] T.A. Holm, T. Bremner, J.B. Newman, Concrete brige decks: lightweight aggregate concrete subject to severe weathering, Concr. Int. 6 (6) (1984) 49-54.

[17] Qingxu Jin, Victor C. Li, Development of lightweight engineered cementitious composite for durability enhancement of tall concrete wind towers, Cement and Concrete Composites, 96, 2019, 87-94.

[18] Z.Y. Huang, J.Y. Wang, J.Y.R. Liew, P. Marshall, Lightweight steel-concrete-steel sandwich shell subject to punching shear. Ocean Eng. 102 (2015) 146-161.

[19] K.S. Chia, X.M. Liu, J.Y.R. Liew, M. H. Zhang, Experimental study on creep and shrinkage of high-performance ultra lightweight cement composite of 60MPa. Struct. Eng. Mech. 50 (5) (2014), 635-652.

[20] Y.P. Wu, J.Y. Wang, P.J. M. Monteiro, M.H. Zhang, Development of ultralightweight cement composites with low thermal conductivity and high specific strength for energy efficient buildings. Constr. Build. Mater. 87 (2015) 100-112.

[21] Z.Y. Huang, J.Y.R. Liew, Compression resistance of steel-concrete-steel composite wall with J-hook connectors. J. Constr. Steel Res. 124 (2016) 142-162.

[22] Z.Y. Huang, J.Y. Wang, J.Y.Richard Liew and Peter Marshall. Lightweight steel-concrete-steel sandwich shell subject to punching shear. Ocean Eng 2015; 102: 146-161.

[23] Z.Y. Huang, J.Y.R. Liew, Structural behaviour of steel-concrete-steel sandwich composite wall subjected to compression and end moment, Thin Wall. Struct. 98 (2016) 592-606.

[24] K.M.A. Sohel, J.Y.R. Liew, Behavior of steel–concrete–steel sandwich slabs subject to impact load. J. Constr. Steel Res. 100 (2014) 163‑175.

[25] D. Fedroff, S. Ahmad, B.Z. Savas, Mechanical properties of concrete with ground waste tire rubber, Trans. Res. Rec. 1532 (1996) 66-72.

[26] G.X. Chen, Impact resistance research on rubberized concrete, Master's Degree Thesis. (2011) (in Chinese).

[27] M.A.E.M. Ali, A.M. Soliman, M.L. Nehdi, Hybrid-fiber reinforced engineered cementitious composite under tensile and impact loading, Mater. Design. 117 (2017) 139-149.

[28] M. Nili, V. Afroughsabet, Combined effect of silica fume and steel fibers on the impact resistance and mechanical properties of concrete. Int. J. Impact Eng. 37 (8) (2010) 879-886.

[29] T. Gupta, R.K. Sharma, S. Chaudhary, Impact resistance of concrete containing waste rubber fiber and silica fume. Int. J. Impact Eng. 83 (2015) 76-87.

[30] F. Liu, G.X. Chen, L. J. Li, Y.C. Guo, Study of impact performance of rubber reinforced concrete, Constr. Build. Mater. 36 (2012) 604-616.

[31] W.H. Feng, F. Liu, F. Yang, L.J. Li, J. Li, Experimental study on the effect of strain rates on the dynamic flexural properties of rubber concrete, Constr. Build. Mater. 224 (2019) 408-419.

[32] A.O. Atahan, U.K. Sevim, Testing and comparison of concrete barriers containing shredded waste tire chips, Mater. Lett. 62 (21–22) (2008) 3754–3757.

[33] S. HentZ, F.V. Donzé, L. Daudeville, Discrete element modelling of concrete submitted to dynamic loading at high strain rates, Comput. Struct. 82 (29) (2004) 2509-2524.

[34] M. Adamu, B.S. Mohammed, M.S. Liew, Effect of crumb rubber and nano silica on the creep and drying shrinkage of roller compacted concrete pavement, Int. J. Goe. 15 (47) (2018) 58-65.

[35] ACI Committee 544, State-of-the-art report on fiber reinforced concrete, American Concrete Institute, Detroit, 1996 Report 544.1R-96.

[36] D.Y. Yoo, N. Banthia, Impact resistance of fiber-reinforced concrete – A review. Cement Concrete Comp. 104 (2019) 103389.

[37] Y.C. Guo, J.H. Xie, W.Y. Zheng, J.L. Li, Effects of steel slag as fine aggregate on static and impact behaviours of concrete, Constr. Build. Mater. 192 (2018) 194-201.

[38] ASTM, C 39/C 39M-18. Standard Test method for compressive strength of cylindrical concrete specimens. West Conshohocken (PA): ASTM International; 2017.

[39] JSCE, Recommendations for Design and Construction of High-Performance Fiber Reinforced Cement Composites with Multiple Fine Cracks, Japan Society of Civil Engineers, Tokyo, Japan, 2008.

[40] J. Hopkinson, On the rupture of iron wire by a blow, in: B. Hopkinson (Ed.), Original papers-by the late John Hopkinson, Scientific Papers, Cambridge Univ. Press, 1901. 316-320.

[41] Y.W. Zhou, B. Xi, K.Q. Yu, et al. Mechanical properties of hybrid ultra-high performance engineered cementitous composites incorporating steel and polyethylene fibers, Mater. 11 (8) (2018) 1448-1468.

[42] T. Ngo, P. Mendis, T. Krauthammer, Behavior of ultrahigh-strength prestressed concrete panels subjected to blast loading, J. Struct. Eng. 2007, 133 (11) (2007) 1582-1590.

[43] Xiong B, Demartino C, Xiao Y. High-strain rate compressive behavior of CFRP confined concrete: Large diameter SHPB tests. Construction and Building Materials, 2019, 201:484-501.

[44] H.Y. Zhou, A. M. Brooks.， D. Hanna, B. Salarieh. Thermal and mechanical properties of cementitious for additive construction of energy-saving habitats, Earth and Space 2018. Cleveland OH， ASCE, (2018) 600-610.